Network Model for the Odor-Specific Temporal Patterns in Locust Olfactory Interneurons

Maxim Bazhenov[1], Mark Stopfer[2], Mikhail Rabinovich[3], Henry D. I. Abarbanel[3,4],
Terrence J. Sejnowski[1,5] and Gilles Laurent[2]

[1]Howard Hughes Medical Institute, The Salk Institute, Computational Neurobiology Laboratory,
La Jolla, CA 92037
[2]California Institute of Technology, Biology Division, 139-74, Pasadena
[3]Institute for Nonlinear Sciences, University of California San Diego, La Jolla, CA 92093-0402
[4]Department of Physics and Marine Physical Laboratory, Scripps Institution of Oceanography,
University of California San Diego, La Jolla, CA 92093-0402
[5]Department of Biology, University of California San Diego, La Jolla, CA 92093

Abstract

Locust antennal lobe projection neurons (PNs) display slow temporal patterns of activity in response to olfactory stimuli. These patterns are composed of 100-200 ms epochs of depolarizing and hyperpolarizing activity, which are stimulus specific and reproducible. Simultaneous recordings from small groups of PNs in the locust antennal lobe also found that they would transiently synchronize during odor responses. Pairwise synchronization (or synchronization to the average local field potential) typically lasted for only a few cycles of the oscillatory population response. The mechanisms underlying these phenomena were investigated here in a model of the antennal lobe using single compartment Hodgkin-Huxley type models of PNs and inhibitory local neurons (LNs). (1) The activation of the slow inhibitory receptors between LNs and PNs produced hyperpolarization and controlled spike activity in ways similar to those observed experimentally. Depending on the temporal patterns of activity in the presynaptic LNs, the hyperpolarization in the PNs lasted from 100 to 400 ms and was stimulus specific. (2) The fine structure of PN spikes was controlled by the fast GABAergic input from presynaptic LNs. Reduction of the fast IPSPs in groups of PNs during specific temporal epochs of stimulation, destroyed the synchrony of oscillations in these neurons. This model predicts that both LN-PN and reciprocal LN-LN inhibitory connections are required for temporal encoding of olfactory information in this system.

INTRODUCTION

A characterization of temporal coding in olfactory systems is slow complex temporal patterns of excitation and inhibition demonstrated by olfactory neurons during stimulus–evoked oscillations. Such patterns have been observed in the olfactory bulbs of amphibians (Kauer, 1974; Kauer and Shepherd, 1977) and mammals (Chaput and Holley, 1980; Meredith, 1986; Meredith, 1992) and in the antennal lobe in insects (Christensen and Hildebrand, 1987). The slow temporal patterns have been shown to be odor specific and reproducible over the trials in locust olfactory system (Laurent and Davidowitz, 1994; Wehr and Laurent, 1996).

Recent intracellular recordings *in vivo* from locust antennal lobe projection neurons (PNs) have revealed that the times during which PNs are phase-locked with population oscillations depend on the presented odor. Thus there is a fine structure to the timing of action potentials in PN oscillations which is also stable over the trials and different for different olfactory neurons (Laurent et al., 1996; Laurent, 1996). This multilevel scheme of odor representation and coding becomes even more complicated considering that different odors evoke responses in spatially different groups of neurons (Laurent and Davidowitz, 1994; Leitch and Laurent, 1996). Thus, odor processing in the locust antennal lobe appears to involve a complex scheme of spatio-temporal coding with odor-specific populations of PNs responding to applied odor with odor- and neuron-specific sequences of temporal firing patterns.

In this paper we analyzed the mechanisms of temporal coding with computational model of antennal lobe neural network. We found that the synchrony of PN oscillations depended on the fast inhibitory input provided by the local neurons (LNs). This input was controlled by the spatio-temporal patters of LN oscillations and its changes were odor-specific. The patterns of LN activity also effected the activation of the slow inhibitory receptors between LNs and PNs, that underlied the appearance of the slow temporal structure of PN responses.

METHODS

Network geometry

We simulated a network of 90 PNs and 30 LNs. For the LN neurons we included a transient Ca^{2+} current I_N (Laurent et al., 1993), a calcium–dependent potassium current $I_{K(Ca)}$ (Sloper and Powell, 1978), a fast potassium current I_K (Traub and Miles, 1991) and a potassium leak current I_{KL}. For the PN neurons we included a fast sodium current I_{Na} (Traub and Miles, 1991), a fast potassium current I_K (Traub and Miles, 1991), a transient potassium A–current I_A (Huguenard et al., 1991) and a potassium leak current I_{KL}. We assumed random (with probability 0.5) interconnections between all neurons. 33% randomly selected LNs and PNs were stimulated by pulses of current as the odor stimulation. These values are higher than those estimated from the experimental data (Laurent, private communication). However the
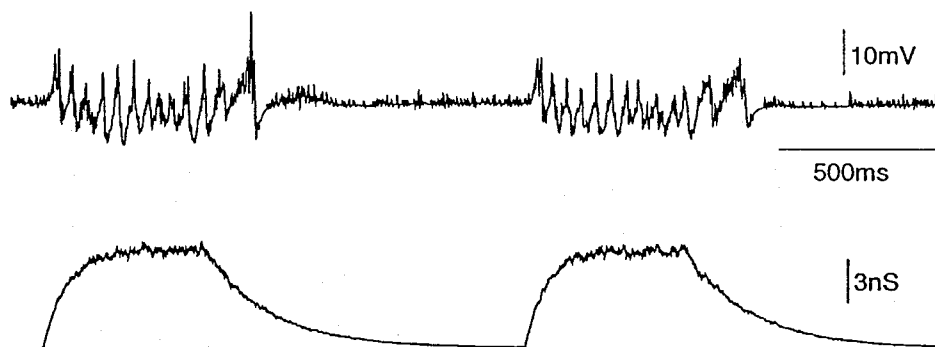
Figure 1: Averaged network activity. During olfactory stimulation (two 500 ms current pulses are showed at the bottom panel) the PN oscillations were synchronized at the frequency about 20 Hz.

choice of these parameters in our model depended on total number of neurons. In a network with number of cells close to *in vivo* data (about 10 times more than in our model (Laurent, 1996)), the probabilities of all interconnections would be rescaled by factor 10.

Some of the intrinsic parameters of the neurons in the network were initialized with random variability to ensure robustness of the results. Small-amplitude current in the form of Gaussian noise (about 10% deviation) was introduced to each cell to achieve random fluctuation of the membrane potential. A stimulus was modeled by a current pulse with a rise time constant α=0.01 ms and decay time constant β=0.005 ms. Gaussian noise (about 10% deviation) was added to the stimulation pulses.

Phase analysis

The averaged PN oscillations (field potential) were low-pass filtered with frequency cut offs at 50 Hz. The PN spikes times were converted to phases. The peaks of the field potential was assigned a phase 0 or 2π and right (left) nearest minimums were assigned a phase $+\pi$ (-π). The phase of each PN spike was calculated relatively to the nearest peak of the field potential (Laurent et al., 1996).

RESULTS

Transient synchronization

To find stimulus–evoked responses in large LN–PN population we simulated network model of 90 PNs and 30 LNs. Without stimulation the neurons displayed spontaneous activity that was not synchronized over the ensemble. When the external stimulus was delivered the network activity was synchronized at about 20 Hz (see Fig. 1).

To investigate the temporal patterns of PN synchronization more precisely phase analysis (see Methods) was used to examine the fine structure and timing of the action potentials during stimulus presentations. The results of this analysis are presented
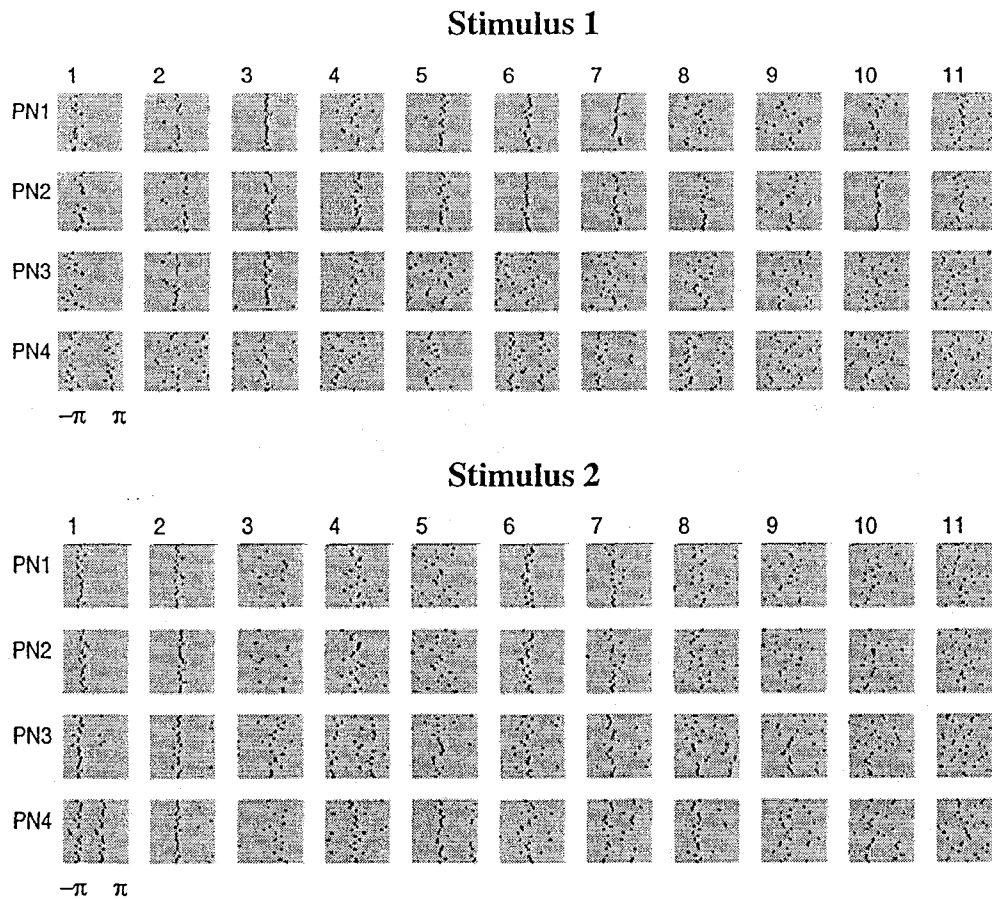
Stimulus 1

Stimulus 2

Figure 2: PN responses for two different stimuli. Four cells (rows) are shown. The response of each cell has been divided into 11 epochs of about 50 ms each. In each epoch the positions of the action potentials relative to the maximum of the average activity were measured. This operation was repeated 20 times for each odor (rasters).

(Fig. 2) for four PNs and two different stimuli. The identical subsets of PNs but different subsets of LNs were stimulated. We found that these stimuli elicited responses in almost identical populations of PNs, while the fine structure of PN synchronization was completely different.

To find a mechanism underlying transient synchronization of PN oscillations we analyzed activity in sets of presynaptic LNs. Fig. 3 shows responses of three PNs for one of the stimuli presented in Fig. 2. For each of these cells we first selected a set of presynaptic LNs. Then for each cycle of oscillations we calculated a total number of Ca^{2+} spikes produced by all presynaptic LNs over the interval between two nearest peaks of field potential at this cycle of oscillations. The number of Ca^{2+} spikes characterized total inhibitory input to the selected PN during each cycle of the stimulus-evoked response. In Fig. 3 the average number of spikes is plotted for all twenty trials. There was a clear correlation between the number of LN spikes and synchrony of PN responses. PN action potentials were phase-locked with the field
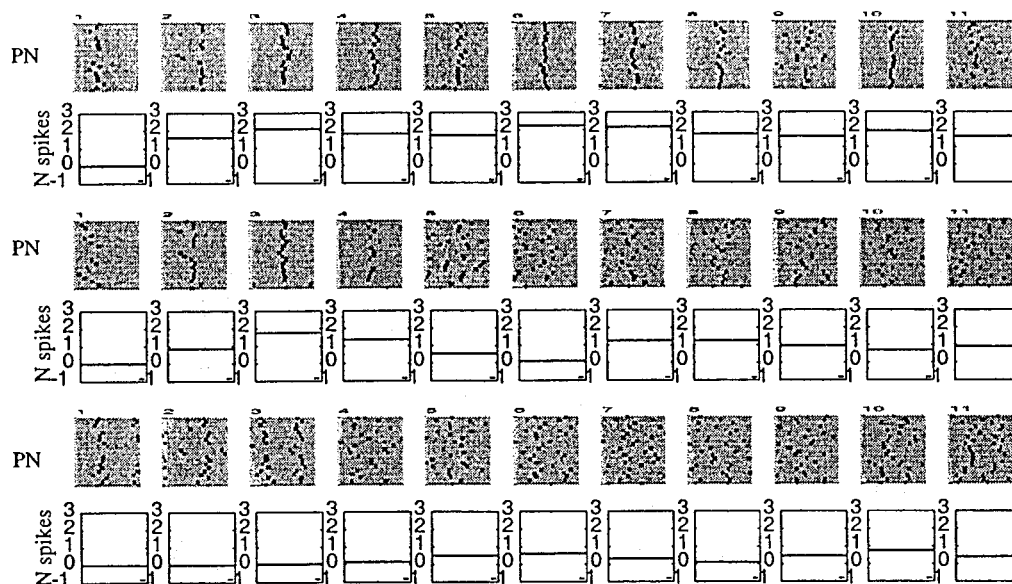
Figure 3: Role of LN inhibition for temporal pattering of PN responses. The responses of three PNs from Fig. 2 are shown (upper panels of each subplot) together with the (averaged over the 20 trials) number of Ca^{2+} spikes in all presynaptic LNs for each cycle of field oscillations (lower panels). The synchrony of PN responses during each cycle of oscillations was strongly correlated with number of preceding LN spikes.

potential when the average number of spikes in all presynaptic LNs was about 2 and desynchronized when it was fewer than one. Thus, changes of fast GABAergic input to PNs can provide a mechanism for transient PN synchronization during stimulus evoked oscillations.

Slow temporal patterns

Fluctuations in the inhibitory input from LNs can explain the appearance of the fine temporal structure of PN synchronization. At the same time, the temporal patterns of PN membrane potentials in this model were almost identical for different stimuli and did not show a complex long-scale temporal structure observed experimentally (Laurent et al., 1996). To examine this we extended our model by including slow inhibitory receptors between LNs and PNs. We required a few presynaptic spikes to occur one after another to activate these receptors, and set the decay time constant to 200-300 ms.

Fig. 4 shows the membrane potentials of a few PNs from a network of 90 PNs and 30 LNs during repetitive presentations of two different stimuli. Each PN displayed specific temporal patterns of depolarizing and hyperpolarizing activity. As for the patterns of transient synchronization, the slow variations of PN membrane potential depended on the spatio-temporal patterns of LN oscillations. Activity increases in some of the LNs during specific epochs of stimulation led to activation of slow inhibitory receptors in the postsynaptic PNs and their hyperpolarizations lasted a few
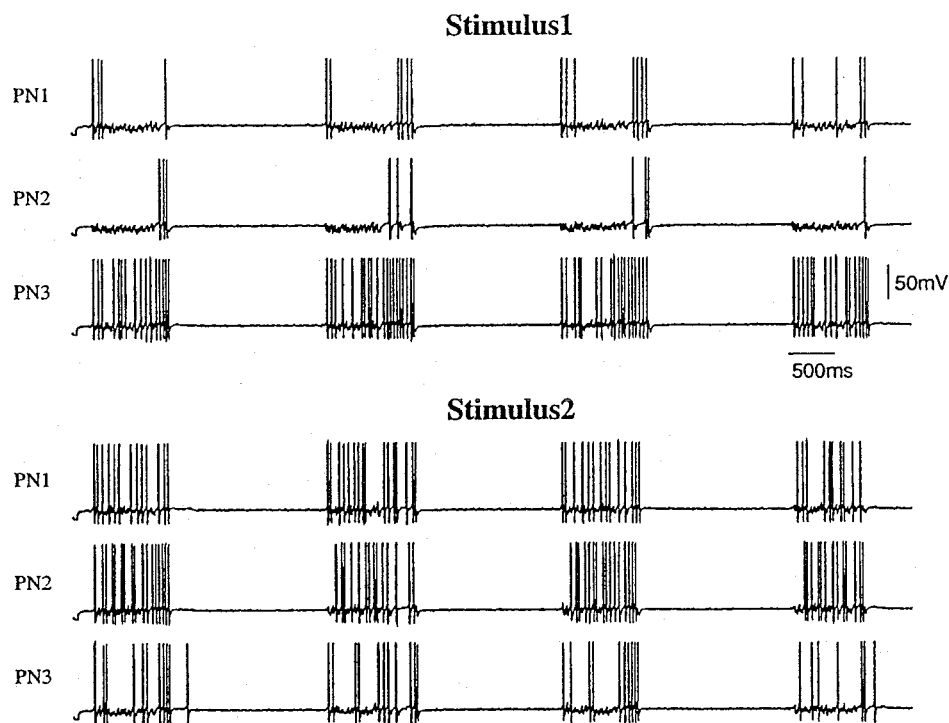
Figure 4: Slow temporal patterns of PN activity. Three PNs are showed during repetitive stimulation (four 500 ms trials separated by 2.5 sec intervals). Different stimuli evoke distinct temporal patterns in olfactory neurons.

hundreds of milliseconds. The input from LNs depended on the applied stimulus, so the slow temporal patterns were stimulus specific and different for different neurons.

We found that many PNs showed an "off-set" depolarization, which was also observed experimentally (see, e.g., Laurent et al., 1996). This effect can be explained by the fast disinhibition of PNs following the stimulus termination. It is important to emphasize that the described temporal patterns of PN activity depended on the slow inhibitory receptors only and remained intact when the fast GABAergic synapses were blocked (not shown). This result is in a good agreement with *in vivo* observations.

CONCLUSION

An antennal lobe network model presented here makes several predictions which can be experimentally tested. First, the synchrony of PN oscillations depends on LN-evoked fast GABA–mediated IPSPs. Odor–specific fine temporal structure of PN responses appeared to result from odor specific spatio-temporal patterning of LN oscillations. These patterns are controlled by the fast inhibitory synapses between LNs. Second, activation of the slow inhibitory synapses between LNs and PNs may explain the appearance of the complex and odor–specific slow temporal structure of

PN responses. Third, while the temporal coding may be unnecessary to discriminate chemically different odorants, such coding becomes important when the presented odors belong to related groups and evoke responses in similar sets of PNs (Stopfer et al., 1997).

References

Chaput M, Holley A (1980) Single unit responses of olfactory bulb neurons to odor presentation in awake rabbits. J Physiol (Paris) 76: 551-558.

Christensen T, Hildebrand J (1987) Male-specific, sex pheromone-selective projection neurons in the antennal lobes of the moth *Manduca sexta*. J Comp Physiol A 160: 553-569.

Huguenard JR, Coulter DA, McCormick DA (1991) A fast transient potassium current in thalamic relay neurons: kinetics of activation and inactivation. J Neurophysiol 66:1305-1315.

Kauer JS (1974) Response patterns of amphibian olfactory bulb neurons to odor stimulation. J Physiol (Lond) 243: 695-715.

Kauer JS, Shepherd GM (1977) Analysis of the onset phase of olfactory bulb unit responses to odour pulses in the salamander. J Physiol (Lond) 272: 495-516.

Laurent G, Seymourlaurent KJ, Johnson K. (1993) Dendritic excitability and a voltage-gated calcium current in locust nonspiking local interneurons. J Neurophysiol 69: 1484-1498.

Laurent G, Davidowitz H (1994) Encoding of olfactory information with oscillating neural assemblies. Science 265: 1872-1875.

Laurent G, Wehr M and Davidowitz H (1996) Temporal representations of odors in an olfactory network. J Neurosci 16: 3837-3847.

Laurent G (1996) Dynamical representation of odors by oscillating and evolving neural assemblies. Trends Neurosci. 19: 489-496.

Leitch B, Laurent G (1996) GABAergic synapses in the antennal lobe and mashroom body of the locust olfactory system. J Comp Neurol 373: 487-514.

Meredith M (1986) Patterned response to odor in mammalian olfactory bulb: the influence of intensity. J Neurophysiol 56:572-597.

Meredith M (1992) Neural circuit computation: complex patterns in the olfactory bulb. Brain Res Bull 29:111-117.

Sloper JJ and Powell TPS (1978) Ultrastructural features of the sensori-motor cortex of the primate. Philos Trans R Soc Lond B Biol Sci. 285: 124-139.

Stopfer M, Bhagavan S, Smith BH, Laurent G (1997) Impaired odour discrimination on desynchronization of odour-encoding neural assemblies. Nature 390:70-74.

Traub RD, Miles R (1991) Neuronal Networks of the Hippocampus. Cambridge: Cambridge University Press.

Wehr M, Laurent G (1996) Odor encoding by temporal sequences of firing in oscillating neural assemblies. Nature 384: 162-166.